Tribology International 60 (2013) 77–82

Contents lists available at SciVerse ScienceDirect

Tribology International

journal homepage: www.elsevier.com/locate/triboint

Short Communication

Dry sliding wear maps for AA7010 (Al–Zn–Mg–Cu) aluminium matrix composite

R.N. Rao [a,*], S. Das [b], D.P. Mondal [b], G. Dixit [c], S.L. Tulasi Devi [d]

[a] Mechanical Engineering Department, National Institute of Technology, Warangal 506 004, A.P., India
[b] Advanced Materials and Processes Research Institute (CSIR, New Delhi), Bhopal 462 026, India
[c] Maulana Azad National Institute of Technology, Bhopal 462 007, India
[d] SOM, National Institute of Technology, Warangal 506 004, A.P., India

ARTICLE INFO

Article history:
Received 4 May 2012
Received in revised form
5 October 2012
Accepted 15 October 2012
Available online 26 October 2012

Keywords:
Wear mechanism map
Mild wear
Severe wear
Aluminium alloy

ABSTRACT

Wear mechanism map for aluminium matrix composite helps in predicting and understanding different wear mechanisms in a material. It also identifies the critical load and sliding speed for transition of one wear mechanism to other. In the present investigation, the wear coefficient is in the range of 10^{-4}–10^{-5} which is at the boundary region between mild to severe wear. It is also observed from that there are four wear regimes; they are ultra mild wear, mild wear or oxidative wear, delamination wear and severe wear. All these facts are discussed on the basis of prevailing wear mechanism.

1. Introduction

Aluminium matrix composites have emerged as advanced materials for several potential applications in automotive, space, aircraft, defence and other engineering sectors [1–6] because of their high specific strength and stiffness, superior wear and seizure resistance as compared to the alloy irrespective of applied load and sliding speed. Attempts have been made to examine the effect of sliding velocity and applied load on the wear behaviour of aluminium alloy and composites. Wilson and Alpas [7] clearly demonstrated the strong interaction between load and sliding velocity in causing wear of a material [8,9]. Wilson and Alpas [7] represented wear mechanism maps for A356 alloy/SiC composites. According to these investigators [7,10–14] four wear regimes were observed in the composites and the alloy depending on speed and applied load. They are mild wear, mixing and oxidative wear, delamination wear and severe wear. Mild wear occurs at a very slow speed and lower applied load. At relatively slower speed, if the load increases considerably, mixing of wear debris and counterface material could take place which due to higher temperature rise, gets oxidized. The oxidized layer may cover the surface and reduce the wear rate. The formation and removal of this layer determines the overall wear rate of the material. This is termed as oxidative wear. At higher load, this layer is easily broken and removed from the specimen surface and thus resulting higher wear rate with applied load and sliding speed. At higher sliding speed, relatively at lower applied load delamination mechanism is prevailing. This may be due to more adiabatic type of heating and cause more adhesive action between the two surfaces. Severe subsurface cracking could take place due to the shear type of deformation of the mixed layer and plastic incompatibility between mixed layer and the underlaying material. The subsurface deformation (which may be the important factor for subsurface cracking) and subsurface microstructural changes have been reported by most of the investigators. Severe subsurface cracking leads to delamination of mixed layer from the wear surface. At a critical applied load and sliding velocity, temperature rises so high and because of severe degree of delaminaiton, mixed layer becomes discontinuous and naked material comes in contact with counter surface. This also leads to a rise in surface temperature to a critical value i.e. flashing temperature at which strong adhesion between counter surface and specimen takes place. This leads to severe wear i.e. onset of seizing.

Several wear mechanisms have been reported in studies of Al and its alloys in dry sliding contact against steel surfaces. The observations of Shivanath et al. [15] are typical. They identified two wear mechanisms in aluminium alloys: one oxidational and the other metallic. In oxidational wear regime, wear rates were low, with the worn surfaces covered by dark compacted transfer

* Corresponding author. Tel.: +91 9441569066; fax: +91 8702459547.
E-mail addresses: rnraonitw@gmail.com, rnrao@nitw.ac.in (R.N. Rao).

0301-679X/$ - see front matter © 2012 Elsevier Ltd. All rights reserved.
http://dx.doi.org/10.1016/j.triboint.2012.10.007

layer, presumed to consist of Al_2O_3 and transferred steel. The onset of metallic wear occurred above a characteristic load at which massive deformation of the aluminium alloy surface occurred, accompanied by the formation of metal fragments which tended to adhere to the steel counter surface. Wear rates in this severe wear regime were at least an order of magnitude greater than those in the mild wear regime; these observations are similar to those of [16–18]. Some controversy exists about the wear mechanisms and exact compositions of the transfer layers formed in the mild wear regime [19,20].

Zhang and Alphas [21] reported that during sliding the exposed portions of these reinforcement particles creates a local abrasive action on the steel counter surface. Wang and Rack [22] studied the wear debris produced by both the composites and unreinforced alloy. In the work by Alpas and Zhang [23], severe wear and seizure was initiated at a load of 98 N and sliding surface bulk temperature of 145 °C in dry sliding wear of aluminum alloy. No severe wear was observed in Al-20vol.% SiC composite, which was tested up to a load of 150 N, at which steady state bulk surface temperatures of 200 °C were measured. Increasing the concentration of reinforcement in an MMC (Metal Matrix Composite) provides better resistance to severe wear. Sliding wear at high speeds has been studied in some detail by Kowk and Lim [24] for Al-based SiC particulate reinforced MMCs. They found that transitions occurred between three regimes with increasing sliding speed. Low speed was characterized by low wear, at higher speed, catastrophic failure occurred at a critical load, resulting in rapid adhesion of MMC material to the counterface; at the highest speeds (29 m/s) extensive melting of the MMC occurred. Under these very severe conditions, the size of the reinforcement particles has a major influence on the wear rate; massive wear will occur if the particles are small. The wear mechanism map also demonstrates that the seizure temperature of A356 alloys (125 °C) is increased significantly by addition of 20% SiC (378 °C). Alpas and Zhang [23] clearly showed schematically how the SiC particles help in forming a mixed layer on the contact surface of composite specimen. Rosenberger [25] studied the mixed layer consisting of matrix material, oxides of matrix material and counter surface, counter surface material and fragmented ceramic reinforcement. The presence of iron and iron oxide has been confirmed by several investigators through XRD (X-ray diffraction) [7,26,22] study or EDX (Energy Dispersive X-ray) analysis [7,14]. Mild and severe wear are derived from the wear mechanism map for steel given by Lim and Ashby [10], these regimes are calibrated against wear rate data to give a wear mechanism map for aluminium alloy and composite.

The wear rate W of a sliding surface is conventionally defined as the volume lost from the surface per unit sliding distance. For a given sliding geometry, it is a function of the normal force, F, acting across the sliding surfaces, their relative velocity, v, their initial temperature, T_o, and thermal mechanical and chemical properties of the materials represented in Eq. (1). One can write

$$W_i = f_i\{F, v, T_o, \text{thermal, mechanical, chemical props.}\} \quad (1)$$

There are number of distinct mechanisms of wear such as plastically dominated wear, oxidation-dominated wear, and melt-dominated wear and so on. Each can be divided into sub mechanisms, mild, severe and oxidational wear. Each mechanism can be described by a normalized wear rate equation of the form given in Eq. (1). Then the dominant mechanism is the one which, for a given F, v, T_o, etc leads to the greatest wear rate. Both the theoretical models suggest that the data from different sources, using specimens of differing shapes and sizes can best be correlated by using a normalized wear rate, force and sliding velocity, defined by the following Eqs. (2)–(4):

$$\overline{W} = W/A_n \quad (2)$$

$$\overline{F} = F/(A_n H_o) \quad (3)$$

$$\overline{V} = (v\, r_o)/a \quad (4)$$

Here 'A_n' is the nominal contact area of the wearing source, 'Ho' is its room-temperature hardness of the softer sliding member, 'a' is the thermal diffusivity and r_o is the radius of the circular nominal contact area. W is the volume lost per unit area of surface, per unit distance slide, F is the nominal pressure divided by the surface hardness: and V can be thought of as the sliding velocity divided by the velocity of heat flow.

In view of the above, in the present study dry sliding wear maps for aluminium matrix composite has been examined under specific applied load and sliding speed. Identifying the critical load and sliding speed for transition of one wear mechanism to other through sliding wear maps gives a better idea to design light weight, high strength, wear and seizure resistance components which are subjected to sliding.

2. Materials and methods

2.1. Material preparation

Aluminium matrix composite was synthesized through solidification processing (stir-casting) route using AA7010 alloy (Al–Zn–Mg–Cu) as matrix and SiC particle (size range: 20–40 μm, wt%: 25) in the present study. The alloy had a chemical composition of Fe—0.27%, Cu—1.28%, Mg—1.14, Zn—5.30% and Al—rest. The composite and the alloy were cast in the form of cylinders of dimension: 200 mm in length and 16 mm in diameter, in a permanent cast iron die. The cast samples were mechanically polished and etched with Keller's reagent (1% HF, 1.5% HCl, 2.5% HNO_3 and remaining water) for microstructural and wear surface observations in SEM (model: JEOL, JSM-5600). The etched samples were sputtered with gold prior to SEM examination.

2.2. Sliding wear tests

Dry sliding wear tests of the alloy and its composite containing 25 wt% SiC particles were carried out using a DUCOM (India) make pin-on-disc machine (Model: TR 2O LE) shown schematically in Fig. 1. Cylindrical test pins (8 mm diameter and 27 mm length) were held against a rotating heat-treated EN32 steel disc conforming to AISI 52100 (1.0%C, 1.4%Cr, 0.40%Mn, 0.2%Si, 0.05%S, 0.05%P and remainder Fe). Hardness of the disc was HRC 65. The steel disc and the samples were polished mechanically up to a roughness (Ra) value of 0.10 μm prior to each test. Wear tests were conducted over a range of applied pressures and sliding speeds. The track diameter of 100 mm, sliding velocities of 0.52, 1.72, 3.35, 4.18 and 5.2 m/s, were used. Load on the specimen was increased in steps until the specimen seized before traversing a fixed sliding distance of 1000 m. Seizure of the specimen was noticed in terms of large material adhesion on to the disc, higher rate of temperature rise of the test pin, and abnormal vibration and noise from the pin-on-disc assembly. Frictional heating was monitored using a chromel–alumel thermocouple inserted in a 1.5 mm diameter hole on the test pin, 1.5 mm away from the sliding surface. The specimens were thoroughly cleaned, dried and weighed prior to and after each test. A Mettler microbalance (Model: H15AR) was used for weighing the specimens. Weight loss was then converted into volume loss per unit sliding distance to compute wear rate.

3. Results and discussion

The microstructure of alloy consists of dendrites of Al and precipitates along the interdendritic regions; micrograph clearly shows the Al dendrites (marked A) and the preicipitates along the dendrite boundaries (arrow marked) in Fig. 2(a). The micrograph of Al–Zn–Mg–Cu–SiC reinforced composite is shown in Fig. 2(b). It clearly shows the uniform distribution of SiC particle in aluminium matrix. Wear phenomena and transitions in wear mechanism over wide ranges of load and sliding speeds were first adopted by Welsh [27] in studies of the sliding wear of mild steel. Schematically it represented different wear mechanism zones on a two-dimensional plot of normalized pressure vs. normalized velocity considered by empirical wear equation, experimentally obtained wear rate and temperature rise. The representation of wear mechanism zone on a paper as a function of applied pressure and sliding velocity for a given material is termed as wear mechanism map. It helps in predicting and understanding different prevailing wear mechanisms in a material under specific applied load and sliding speed. It also helps in identifying the critical load and sliding speed for transition of one wear mechanism to other. Alpas and Zhang [23] investigated wear mechanism map for Aluminum alloys using sliding wear equation for seizure and flash temperature close to T_m leading to transition from mild wear to severe wear. Several investigators have also expressed the severity of the wear from the calculation of wear coefficient. An attempt has been made to analyze the results expressed by Archard's wear equation which predicts that, the wear rate of a material is directly influenced by external variables, such as load, sliding distance, and sliding velocity. The wear rate evaluated using a wear equation based on the work of Archard [28] is given by Eq. (5).

$$Q = KW/H \tag{5}$$

Where, Q is the volume removed from the surface by wear per unit sliding distance, H, the indentation hardness of the softer surface, W is the normal pressure applied between the surface and K Archard's wear coefficient, a dimensionless number which is less than unity. The value of K provides valuable means of comparing severity of different wear processes. For sliding wear of metals typical values of K for the mild wear of metals are 10^{-4} to 10^{-6}, while K becomes 10^{-3} to 10^{-2} for severe wear. An attempt is also made to test the wear equation proposed by Lim and Ashby [10] for seizure, oxidation-dominated wear, severe oxidational wear. One of equations proposed by Lim and Ashby, the Eq. (6) of the seizure is given by

$$\overline{F} = 1/(1+\alpha_t\mu^2)^{1/2}[1-(T_b-T_o)/20T_m\ln 10^6/\beta\,\overline{v}] \tag{6}$$

where, F is the normalized pressure, α_t is the heat distribution coefficient, μ is the coefficient of friction, T_b is the bulk temperature (°C), T_o is the initial temperature (°C), T_m is the melting temperature (°C), β is the dimensional parameter for bulk heating, and $\overline{v}$ is the sliding velocity (m/s). It has been proposed by these investigators that the ranges of normalized wear rate or wear coefficient for different wear mechanisms are for mild and severe wear are 10^{-4}–10^{-6}, and 10^{-3}–10^{-2} respectively. In the present study normalized wear rate for the investigated material under different load and sliding speeds were calculated and it varies in the range of 10^{-4}–10^{-5}. However, it was found that within the selected range of applied load and sliding speed, the investigated materials get seized and the normalized pressure $\overline{F}$ for seizure point was found to be almost 1, which is in good agreement with the theoretical value of $\overline{F}$. Thus there is a possibility of transition of different wear mechanisms from one to the others within the selected applied load and sliding speed. The prevailing wear mechanism such as mild wear, severe wear and seizure were experimentally identified through microscopic observation, EDX analysis and X-ray diffraction studies of worn surface and subsurface [3]. Thus the construction of wear mechanism map only by considering the wear coefficient may not be appropriate. In the present studies the wear coefficient is in the range of 10^{-4}–10^{-5} which is at the boundary region between mild to severe wear. In the present study the wear coefficient of the order of 10^{-5} is considered as mild wear and 10^{-4} as severe wear, evident from worn surfaces observation in SEM analysis [Fig. 5a–d]. The basic steps used in generating wear mechanism maps in the present investigation are

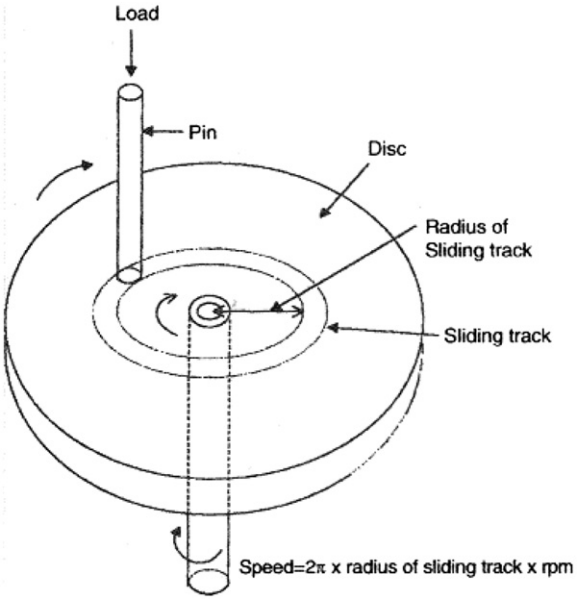

Fig. 1. Schematic diagram of pin-on-disc test set up.

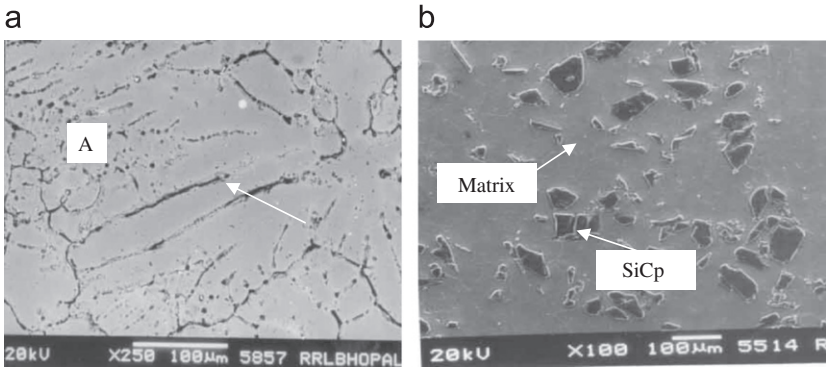

Fig. 2. Scanning electron micrograph of (a) Al–Zn–Mg–Cu alloy and (b) composite showing uniform distribution of SiC particles in aluminium matrix.

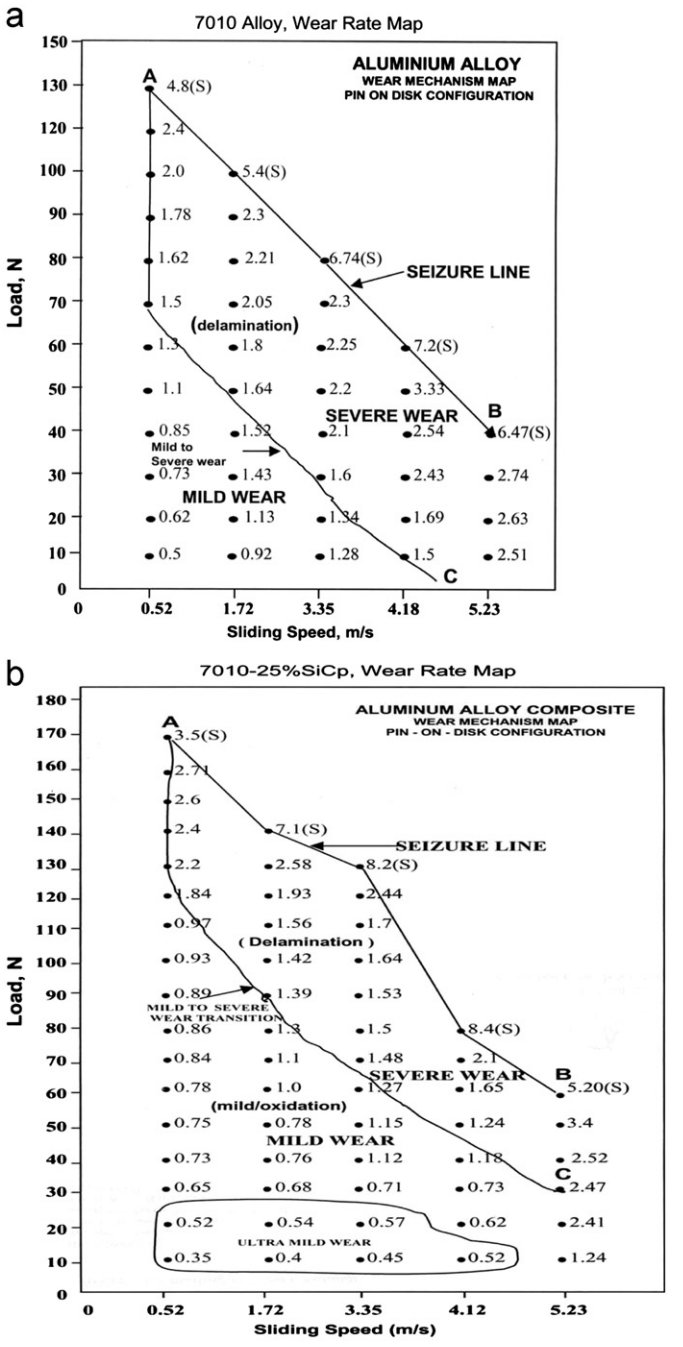

Fig. 3. Wear mechanism map (a) wear rate map for 7010 Alloy (b)wear rate map for 7010–25% SiCp.

(i) recording of wear data and temperature rise from experiments conducted under different applied loads and sliding speeds (ii) microscopic observation of wear surface and identification of wear mechanism (iii) presenting the wear and temperature data in a two-dimensional plane of load and sliding speed and (iv) demarcation line on the plane to separate different wear mechanism zones, considering the value of wear coefficient, worn surface characteristics.

The wear mechanism map for 7010 alloy is shown in Fig. 3(a). It represents the variation of wear rate as a function of load and sliding speed for different wear mechanisms such as mild wear, severe wear (delamination) and seizure. This figure demonstrates that the mild wear is prevailing at lower applied load and sliding speed. At a sliding speed of 0.52 m/s, the mild wear region is extended up to applied load of 60 N and at the same time an applied load of 10 N the mild wear region exists up to sliding speed of 4.18 m/s. The line 'AB' represents the demarcation line for delamination to seizure transition. The applied load and sliding speed below this line does not lead to seizure of the alloy, it thus shows that the alloy seizes at a speed of 0.52 m/s, when the load is 130 N or grater. It also shows that the alloy does not seize when the applied pressure is less than 40 N, even at a sliding speed of 5.23 m/s. The seizure pressure decreases with increasing sliding speed. Line 'AC' represents the transition load and sliding speed for the transition of mild wear to delamination wear. This line follows a parabolic trend and represents the transition load and sliding speed or influenced by each other for transition of mild wear to delamination wear. The critical load decreases with increase in sliding speed. It is interesting to note that the alloy shows a wide region for delamination wear. Fig. 4(a) shows the temperature map for alloy, the demarcation line is made on the

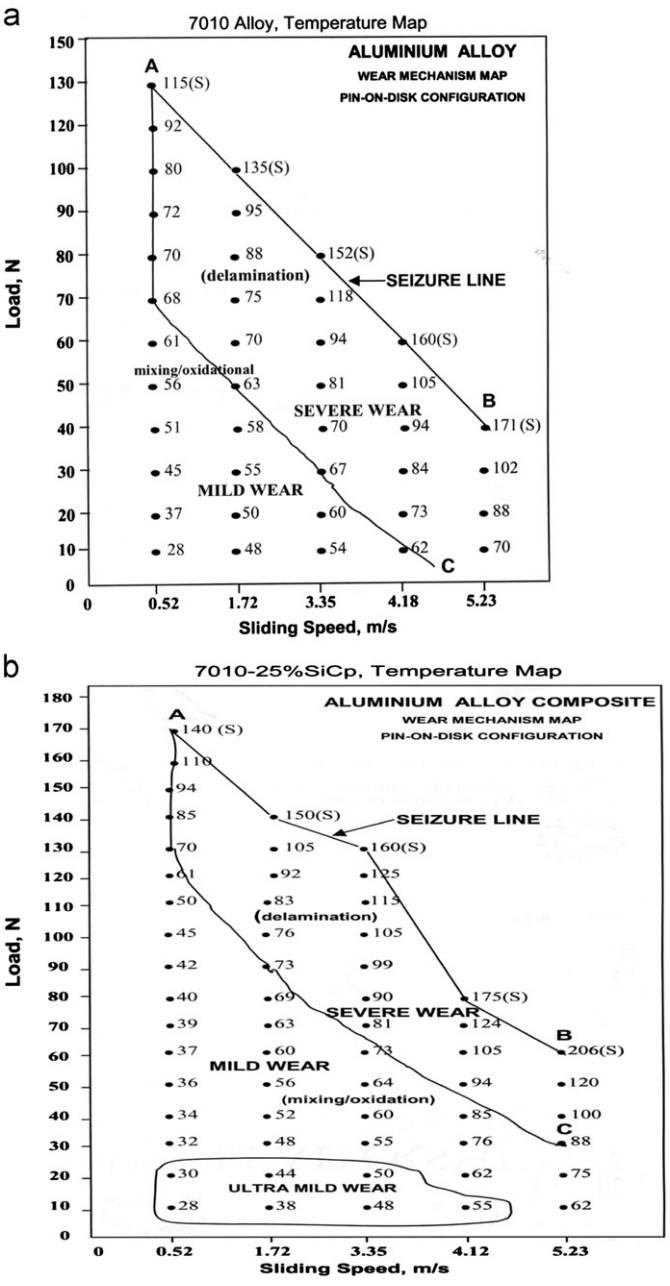

Fig. 4. Wear mechanism map (a) temperature map for 7010 Alloy (b) temperature map for 7010–25% SiCp.

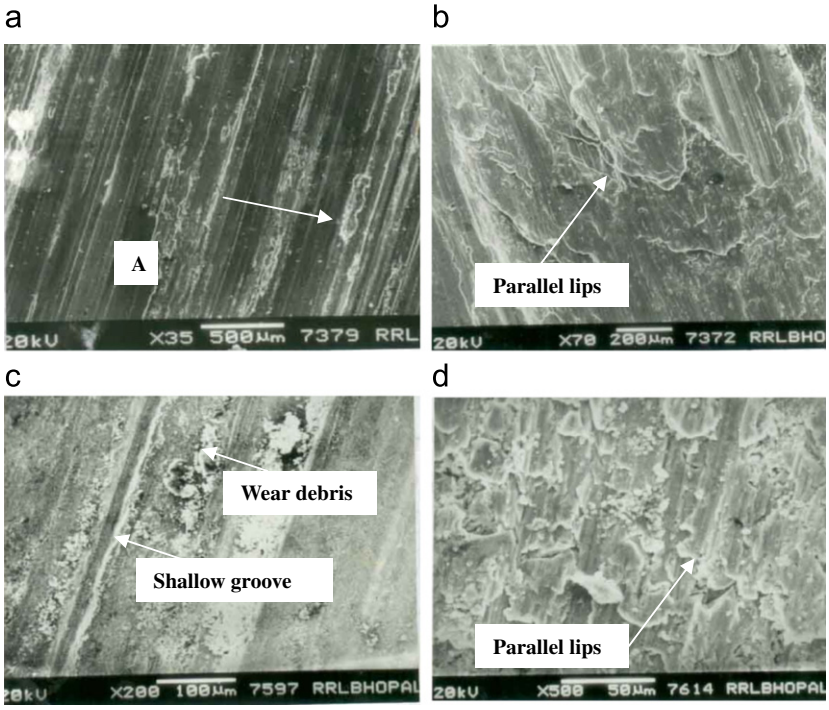

Fig. 5. Typical scanning electron micrograph of worn surface of (a) alloy at lower applied pressure (b) alloy at seizure pressure (c) composite at lower applied pressure and (d) composite at seizure pressure.

temperature plot corresponding to the lines drawn on wear rate map. This figure thus demonstrates that the material undergoes transition from mild wear to severe wear when temperature rise is above 60 °C and seizure takes place when the temperature rise is grater than 115 °C. These data are in good agreement with the seizure temperature for the Al alloy as reported by Alpas and Zhang [16]. Fig. 3(b) shows the wear mechanism for the composite under study. It is seen that the seizure line i.e 'AB' shifted upwards signifying that the composite needs higher applied load, higher sliding speed as compared to the alloy for seizure. The line 'AC' demonstrates the transition load and sliding speed for the transition of mild wear to severe wear and it signifies that this transition load and sliding speed for composite is higher than that of the alloy. The region between 'AB' and 'AC' of composite is narrower as compared to that noted in case of alloy. This signifies that the transition of mild wear to severe wear starts at higher load and sliding speed in composite. The temperature map for this composite was made following the same demarcation line used in wear rate map and is shown in Fig. 4(b). It is seen that the composite get seized at a temperature of 135 °C or higher and the delamination wear starts when temperature is grater than 90 °C. This signifies that composite can withstand higher temperature for seizure as well as transition of wear from mild to delamination. The figure also shows the region corresponds to the ultra mild wear at lower applied load and sliding speed. This is attributed to the protection offered by protruded SiC particle against the effective contact of hard asperities of counter surface. This region is represented primarily by rubbing type of wear.

Fig. 5(a) shows micrograph of AA 7010 alloy, the wear surface is depicted as deeper grooves (marked 'A') and patches of damaged regions (arrow marked). The surface damage is resulted because of nucleation of cracks and their propagation along the grooves. Micrograph of alloy (Fig.5b) shows seized surface, which is characterized by formation of parallel lips (arrow marked) along the wear scar. Typical scanning electron micrograph of the wear surface of 7010–25 wt% SiC particle reinforced composite is characterized by shallow grooves and the surface is covered with

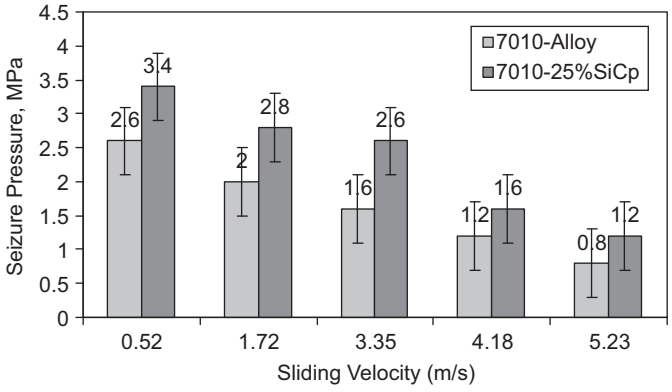

Fig. 6. Seizure pressure as a function of sliding velocity.

Table 1
Comparison of wear mechanism map in terms of seizure load, transition load and transition temperature.

	Seizure load (*N*)		Transition load Mild to severe			Transition temperature Mild to severe		
Material (m/s)	0.52	5.23	0.52	3.35	5.23	0.52	3.35	5.23
Alloy	130 N	40 N	70 N	30 N	–	68 °C	68 °C	–
25% SiCp	170 N	60 N	130 N	90 N	30 N	80 °C	81 °C	88 °C

formation of equiaxed debris shown in Fig.5c. Scanning electron micrograph of composite at seized condition (Fig.5d) is signified by the formation of parallel lips (arrow marked) along the wear scar. Fig. 6 shows the bar chart of seizure pressure as a function of sliding velocity for investigated materials. It indicates that the seizure pressure improved significantly on the addition of SiCp reinforcement to the alloy. It may be noted that the seizure pressure decreases as the sliding velocity increases irrespective of the material. There is a 30–50% improvement in seizure pressure

noticed by addition of SiC particles to the matrix alloy. Highest seizure pressure was noted at lower sliding velocity of 0.52 m/s, reverse is true for sliding velocity of 5.23 m/s.

The comparison of wear mechanism map for the alloy and composite is summarized in terms of transition load and sliding speed for mild to severe wear and seizure in (Table 1). The temperatures corresponding to different demarcation lines are also indicated.

4. Conclusions

1. Wear mechanism maps for Al-alloys and composites are constructed on the basis of wear rates and temperature rise.
2. The wear map of composite is subdivided in three zones, they are ultra mild, oxidation and mechanical mixing mild wear and delamination wear demarcated by boundary lines.
3. Alloy exhibits two wear mechanism zones which are mild wear (oxidation/mechanical mixing) and delamination wear (severe wear).
4. Reliability of sliding wear test procedure was examined by comparing the measured wear rate data with calculated wear rate. It is noted that the measured values are in good agreement with the theoretically calculated value.

References

[1] Rohatgi PK. Metal matrix composites. Journal of Defence Science 1993;43:323–49.
[2] Nussbaum AI. New applications for aluminium based metal matrix composites. Light Metal Age 1997:54–8.
[3] Mondal DP, Das S, Rao RN, Singh M. Effect of SiC addition and running-in-wear on the sliding wear behaviour of Al–Zn–Mg aluminium alloy. Materials and Science Engineering A 2005;40(1–2):307–19.
[4] Rao RN, Das S, Mondal DP, Dixit G. Dry sliding wear behaviour of cast high strength aluminium alloy (Al–Zn–Mg) and hard particle composites. Wear 2009;267:1688–95.
[5] Qin QD, Zhao YG, Zhou W. Dry sliding wear behavior of Mg_2Si/Al composites against automobile friction material. Wear 2008;264:654–61.
[6] Mandal A, Murty BS, Chakraborty M. Sliding wear behaviour of T6 treated A356–TiB2 in-situ composites. Wear 2009;266:865–72.
[7] Wilson S, Alpas AT. Wear mechanism maps for metal matrix composites. Wear 1997;212:41–9.
[8] Perrin C, Rainforth WM. The effect of alumina fibre reinforcement on the wear of an Al-4.3% Cu alloy. Wear 1995;181–183:312–24.
[9] How HC, Baker TN. Characterization of sliding friction-induced subsurface deformation of Saffil-reinforced AA6061 composites. Wear 1999;232:115.
[10] Lim SC, Ashby MF. Wear mechanism maps. Acta Metal 1987;35(1):1–24.
[11] Antoniou R, Subramanian C. Wear mechanism map for aluminium alloys. Scripta Metallurgica 1988;22:809–14.
[12] Lim SC, Ashby MF, Brunton JH. Wear-rate transitions and their relationship to wear mechanisms. Acta Metallurgica 1987;35:1343–8.
[13] Wilson S, Alpas AT. Thermal effects on mild wear transitions in dry sliding of an aluminium alloy. Wear 1999;225–229:440–9.
[14] Chen H, Alpas AT. Sliding wear map for the magnesium alloy, Mg–9Al–0.9Zn (AZ91). Wear 2000;246:106–16.
[15] Shivanath R, Sengupta PK, Eyre TS. The mechanisms of wear. The British Foundry Man 1977;70:349–56.
[16] Hirst W, Lancaster JK. Surface film formation and metallic wear. Journal of Applied Physics 1956;27:1057–65.
[17] Mohammed Jasim K, Dwarkadasa ES. Wear in Al–Si alloys under dry sliding conditions. Wear 1987;119:201–5.
[18] Somi Reddy A, Pramila Bai BN, Murthy KS, Biswas SK. Wear and seizure of binary Al–Si alloys. Wear 1994;171:115–27.
[19] Pramila Bai BN, Biswas SK. Characterization of dry sliding wear of Al–Si alloys. Journal of American Society of Lubrication Engineering 1987;43:57–61.
[20] Clarke J, Sarkar AD. Wear characteristics of as-cast binary aluminium–silicon alloys. Wear 1979;54:7–16.
[21] Alpas AT, Zhang J. Wear regimes and transitions in Al_2O_3 particulate reinforced aluminum alloys. Materials and Science Engineering 1993;A161:273–84.
[22] Wang A, Rack HJ. Abraisve wear of silicon carbide particulate and whisker-reinforced 7091 aluminium matrix composites. Wear 1991;146:337–48.
[23] Alpas AT, Zhang J. Wear rate transition in cast aluminum–silicon alloys reinforced with SiC particles. Scripta Metallurgica 1992;26:505–9.
[24] Kowk JKM, Lim SC. High speed tribological properties of Al/SiC composites: I frictional and wear rate. Composite Science and Technology 1999;59:55–63.
[25] Rosenberger MR, Schvezov CE, Forlerer E. Wear of different aluminum matrix composites under conditions that generate a mechanically mixed layer. Wear 2005;259:590–601.
[26] Venkataraman B, Sundararajan G. The sliding wear behaviour of Al–SiC particulate composites. II. The characterization of subsurface deformation and correlation with wear beaviour. Acta Matallurgica et Materialia 1996;44:461–73.
[27] Welsh NC. The dry wear of steels. Part I. The general pattern of behaviour. Proceedings Royal Society 1965;A257:31–50.
[28] Archard JF. Contact and rubbing of flat surfaces. Journal of Applied Physics 1953;24:981–8.